*J Neurophysiol* 99: 2821–2832, 2008.
First published March 19, 2008; doi:10.1152/jn.01014.2007.

# Whisker Movements Evoked by Stimulation of Single Motor Neurons in the Facial Nucleus of the Rat

**Lucas J. Herfst[1,2] and Michael Brecht[1,2]**

[1]*Bernstein Center for Computational Neuroscience, Humboldt University Berlin, Berlin, Germany; and* [2]*Department of Neuroscience, Erasmus University Medical Center Rotterdam, Rotterdam, The Netherlands*

Submitted 12 September 2007; accepted in final form 13 March 2008

**Herfst LJ, Brecht M.** Whisker movements evoked by stimulation of single motor neurons in the facial nucleus of the rat. *J Neurophysiol* 99: 2821–2832, 2008. First published March 19, 2008; doi:10.1152/jn.01014.2007. The lateral facial nucleus is the sole output structure whose neuronal activity leads to whisker movements. To understand how single facial nucleus neurons contribute to whisker movement we combined single-cell stimulation and high-precision whisker tracking. Half of the 44 stimulated neurons gave rise to fast whisker protraction or retraction movement, whereas no stimulation-evoked movements could be detected for the remainder. Direction, speed, and amplitude of evoked movements varied across neurons. Protraction movements were more common than retraction movements ($n = 16$ vs. $n = 4$), had larger amplitudes (1.8 vs. 0.3° for single spike events), and most protraction movements involved only a single whisker, whereas most retraction movements involved multiple whiskers. We found a large range in the amplitude of single spike-evoked whisker movements (0.06–5.6°). Onset of the movement occurred at 7.6 (SD 2.5) ms after the spike and the time to peak deflection was 18.2 (SD 4.3) ms. Each spike reliably evoked a stereotyped movement. In two of five cases peak whisker deflection resulting from consecutive spikes was larger than expected when based on linear summation of single spike-evoked movement profiles. Our data suggest the following coding scheme for whisker movements in the facial nucleus. *1*) Evoked movement characteristics depend on the identity of the stimulated neuron (a labeled line code). *2*) The facial nucleus neurons are heterogeneous with respect to the movement properties they encode. *3*) Facial nucleus spikes are translated in a one-to-one manner into whisker movements.

## INTRODUCTION

The facial vibrissae function as important tactile sensors in rats (Brecht et al. 1997; Vincent 1912) and rats constantly engage in exploratory whisker movements. With respect to angular speed and repetition rate rodent whisker movements are among the fastest motor patterns generated by mammals. After the initial description of whisking movements (Welker 1964) improvements in high-speed recording techniques have greatly facilitated the analysis of vibrissal motor control (Carvell and Simons 1990; Kleinfeld et al. 1999, 2006; von Heimendahl et al. 2007). Whisking movements are frequency and amplitude modulated during discriminative whisking and movement patterns vary with performance (Carvell and Simons 1995). Whisking movements are not required for all types of discrimination tasks (Krupa et al. 2001), but are essential for horizontal localization tasks and allow rats to encode horizontal object location with great accuracy (Knutsen et al. 2006).

The vibrissal system offers several advantages for the analysis of motor control (Brecht et al. 2006): *1*) movement characteristics of individual whiskers are simple and can be tracked with high precision; *2*) load plays a subordinate role; *3*) whiskers can be easily manipulated; *4*) miniature whisker movements persist even during anesthesia- or sleep-induced paralysis; and *5*) vibrissal motor representations are very large in the rodent brain.

Two classes of muscles generate rhythmic whisker movements: the intrinsic and extrinsic muscles, whose consecutive contractions cause whisker protraction and retraction, respectively (Berg and Kleinfeld 2003a,b; Dörfl 1982). The intrinsic whisker musculature consists almost exclusively of fast contractible, fast fatigable muscle fibers and forms the structural basis for the extraordinary speed of whisker movements (Jin et al. 2004).

The cholinergic motor neurons of the lateral facial nucleus are the sole output station innervating whisker muscles. Most studies on vibrissal motor control focused on motor centers upstream from the facial nucleus. Brain stem circuits were identified that may form a central pattern generator for whisking (Cramer et al. 2007; Hattox et al. 2002, 2003) and numerous studies address the role of vibrissa motor cortex (Ahrens and Kleinfeld 2004; Berg and Kleinfeld 2003b; Brecht et al. 2004; Haiss and Schwarz 2005; Hall and Lindholm 1974). However, little or nothing is known about the impact of single motor neurons on motor output (Porter and Lemon 1993). Facial nucleus cells are large neurons, with dendrites extending beyond the facial nucleus (Friauf 1986). In each half of the brain there are about 1,000 to 2,000 facial nucleus vibrissa motor neurons: according to retrograde tracing experiments 50 to 100 neurons innervate the intrinsic muscles of each macrovibrissa (Klein and Rhoades 1985). The facial nucleus constitutes a bottleneck in vibrissa motor control, which contains orders of magnitude fewer neurons than upstream motor structures like the motor cortex, which may consist of approximately one million neurons (Brecht et al. 2004). Stimulation of the facial nerve elicits whisker protractions tightly locked to the stimulus across a broad frequency range (Lang et al. 2006). To determine how individual facial nucleus motor neurons contribute to whisker movements we combined single-cell stimulation in the rat facial nucleus and high-precision whisker tracking. We find that motor neuron activity is translated spike by spike into fast whisker movements,

Address for reprint requests and other correspondence: L. J. Herfst, BCCN, Humboldt University Berlin, Philippstr. 13 House 6, 10115 Berlin, Germany (E-mail: lucas.herfst@bccn-berlin.de).

The costs of publication of this article were defrayed in part by the payment of page charges. The article must therefore be hereby marked "*advertisement*" in accordance with 18 U.S.C. Section 1734 solely to indicate this fact.

whose direction, speed, and amplitude vary with the identity of the stimulated neuron.

## METHODS

### *Surgery*

All experimental procedures were carried out according to Dutch guidelines on animal welfare under the supervision of a local ethics committee. Standard surgical and electrophysiological techniques were used (Brecht et al. 2004). Animals ($n$ = 58) were anesthetized with ketamine hydrochloride [90 mg/kg, administered intraperitoneally (ip)]/xylazine (5 mg/kg, ip; Alfasan International, Woerden, The Netherlands) for surgical anesthesia. At 45–60 min after the start of surgery animals received supplemental doses of ketamine (20–25 mg/kg) and acepromazine (0.02 mg/kg) as needed [interval ~10 min, supplements (20–33% of the initial dose) administered ip via a small infusion needle]. Rats were placed in a stereotaxic surgical apparatus (Narishige, Tokyo). Depth of anesthesia was regularly monitored by testing hindlimb reflex and vibrissae movements; body temperature was maintained at 37°C. The top of the head was shaved, the skin was infused with lidocaine, and we made a midline skin incision. An oval hole was drilled into the skull (~1.5 × 3 mm, major axis in rostrocaudal direction), vertically above the facial nucleus at about 10.5 mm posterior of bregma, 2.4 mm lateral of midline, left hemisphere. For antidromic stimulation another skin incision was made, exposing a small part of the buccal branch of the left facial nerve (Fig. 1). The appropriate site of exposure was determined by using two projection lines: a vertical line running downward, starting 2 mm posterior from the outer corner of the eye, and a horizontal line running in caudal direction,

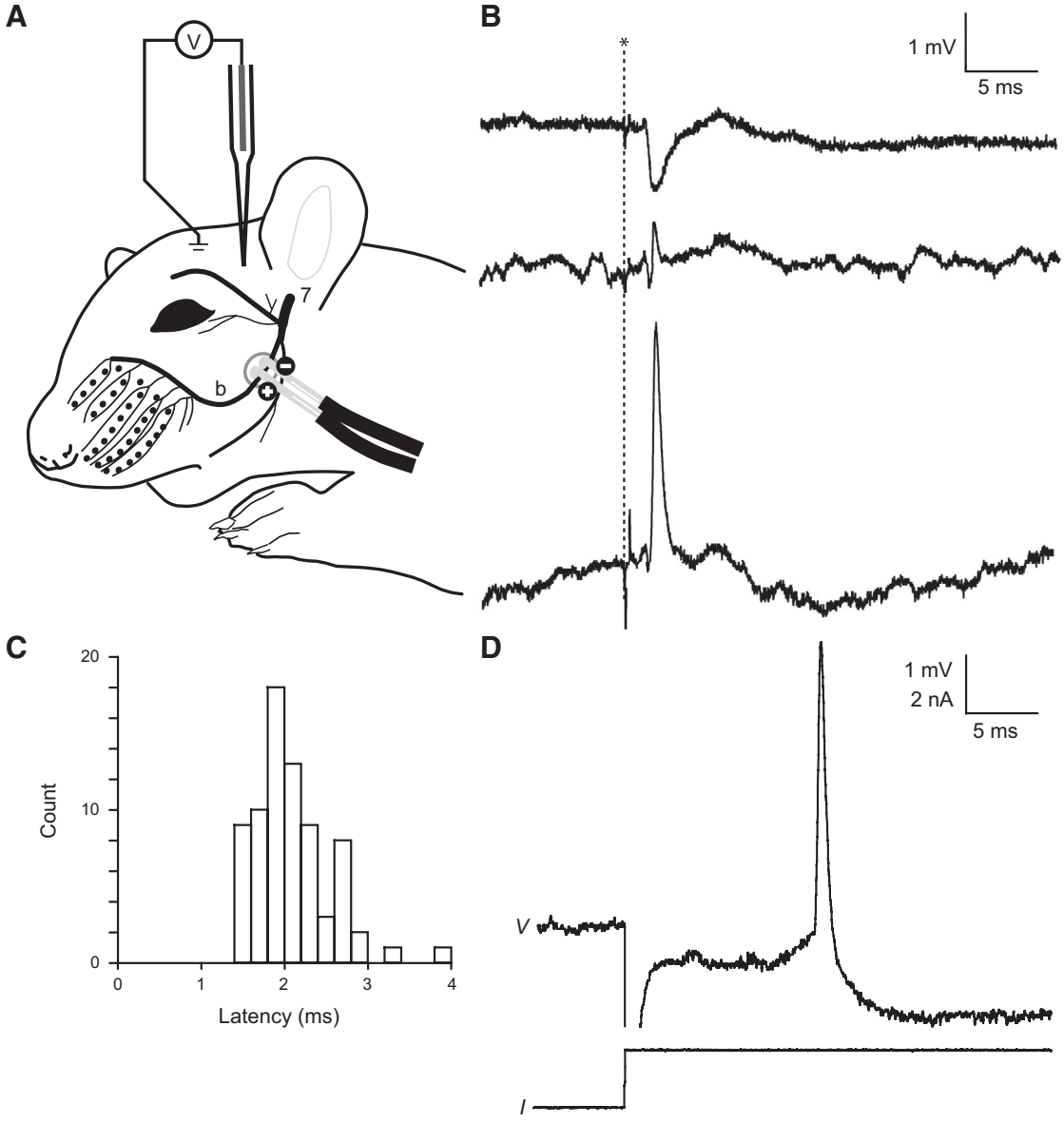


FIG. 1. Antidromic and orthodromic stimulation of vibrissa motor neurons. *A*: recording configuration. An antidromic impulse is evoked in the buccal branch "b" of the 7th nerve. The antidromic signal is then recorded in the facial nucleus. *B*: recording of local field potentials (LFPs) and spikes in the facial nucleus. A temporal change in LFP emerges about 1.4 ms after stimulation (*) and reaches its peak value after about 2.1 ms (*top trace*). A motor neuron close to the pipette tip is detected by its antidromically evoked spike (*middle trace*). The spike grows further in size over time, indicating a transition to a juxtacellular configuration (*bottom trace*). *C*: population histogram of antidromic spike latencies. *D*: spike evoked in response to a constant depolarizing current pulse. Stimulation artifacts have been partially removed.

starting at the whisker E-row. Then two insulated silver wires were hooked and placed around the nerve separated about 2 mm from one another, exposing 2 mm of the wire endings.

### *Electrophysiology*

In initial experiments microstimulation was applied to identify the facial nucleus. A glass pipette electrode was advanced into the brain toward the facial nucleus, posterior 10–11.5 mm and lateral 2.2–2.6 mm relative to bregma, and about 8 mm below the cerebellar surface. Microstimulation was effective in evoking whisker movements, independent of depth of anesthesia. For short volleys of pulses (10 pulses applied at a rate of 100 Hz, 0.3-ms pulse width) we typically observed a stimulation threshold of about 5 $\mu$A for evoking whisker movements. In subsequent experiments, the buccal branch of the facial nerve was electrically stimulated to generate an antidromic signal (Fig. 1). Current was generated by a constant-current stimulus isolator (model A365, World Precision Instruments, Sarasota, FL) and delivered by two chlorided hook-shaped silver wires placed over the buccal branch of the left facial nerve. Stimulation consisted of 0.3-ms-long monophasic cathodal single current pulses of 0.8–2 mA amplitude at a rate of 0.33 Hz. Stimulation currents of 0.8 mA were sufficiently large in the majority of experiments. Stimulation of the buccal branch of the facial nerve gave rise to protractions in the left whisker pad and—according to the intention of antidromic identification of motor neurons—it was set up such that it would be saturating and activating all facial motor neurons. To achieve this goal we increased the current until a maximal movement was observed and we also regularly verified that increasing stimulation current did not evoke an increasing local field potential (LFP) response. In vivo juxtacellular recordings were made as described previously (Pinault 1996). The electric signal was low-pass filtered at 3 kHz by a patch-clamp amplifier (model BVC-700A, Dagan, Minneapolis, MN), then sampled at 10 or 20 kHz by an LIH 1600 acquisition interface (HEKA Elektronik, Lambrecht, Germany) under the control of Patchmaster software (HEKA Elektronik). Patch pipettes (4–6 M$\Omega$) were used with an outer diameter of 1.5 mm pulled from borosilicate filamented glass capillaries on a horizontal puller (P-97 Flaming/Brown Micropipette Puller, Sutter Instrument, Novato, CA). Pipettes were filled with (in mM): 135 K-gluconate, 10 HEPES, 10 $Na_2$-phosphocreatine, 4 KCl, 4 MgATP, 0.3 $Na_3GTP$, and 20 mg/ml biocytin, pH adjusted to 7.2. Ringer solution (135 NaCl, 5.4 KCl, 1.0 $MgCl_2$, 1.8 $CaCl_2$, 5.0 HEPES, pH 7.2) was applied to the brain surface. Pipettes had a relatively long and thin taper and a blunt cone-shaped tip with a high cone angle, thus minimizing tissue damage and compression. Single units were searched for by advancing the tip of the recording electrode with 2-$\mu$m steps, while stimulating the buccal branch of the facial nerve and monitoring changes in the population field response and the presence of antidromic spikes within 4 ms poststimulus. On detection of small extracellular action potentials ($<$1 mV), the electrode was carefully advanced further. The juxtacellular recording mode was evident from an increased baseline noise level, an increase in series resistance, or the presence of spikes with amplitudes $>$2 mV. Once the juxtacellular recording mode was obtained, brief current pulses (150–200 ms) were applied through the micropipette to excite the recorded neuron. All voltage recordings of stimulation experiments were visually inspected for (evoked) spikes. Spike time and spike amplitude were determined by a threshold-crossing technique. The threshold value was set at twice the peak-to-peak noise level in 5-ms time frames. To assess whether indeed single neurons were stimulated all traces were checked for the presence of secondary units. With respect to secondary units we refer to spike waveforms in our recordings that are different from the spike waveform of the target neuron.

### *Whisker video tracking*

The whisker area was videotaped from the top and whiskers were observed under a stereomicroscope to detect even the smallest whisker movements. Timing of the pulses was visualized by placing a light-emitting diode light in the field of view, which was controlled by TTL inputs from the current signal. At the same time we gradually increased the electric current pulse amplitude until spikes were elicited. Electric current strength was regularly adjusted close to or above spiking threshold to prevent cell damage. Once whisker movements were detected, the respective whisker(s) was labeled with reflective foil. In a subset of cases ($n = 6$) the movements were then recorded by a digital high-speed camera (model MV-D640-66-CL10, Photon Focus, Lachen SZ, Switzerland), at high frame rates ($\geq$200 frames/s). Depending on actual experimental conditions, the frame rate was set to a value that best met the requirements of high temporal and spatial resolution. In all other cases movements were documented on DVD at video rate (50 Hz deinterlaced). Angular movements of the labeled whiskers were quantified and related to the current pulses and spike times using custom software developed under LabVIEW (National Instruments, Austin, TX). Next, physiologically identified responsive cells were juxtacellularly labeled using continuous trains of current pulses (Pinault 1996).

### *Histology*

At the end of recording, the animal was injected with an overdose of ketamine and then perfused transcardially with 0.1 M phosphate-buffered saline followed by a 4% paraformaldehyde solution. The brain was removed, stored overnight in a 10% sucrose solution, embedded in gelatin, frozen, and sectioned into 80-$\mu$m-thick coronal slices. Slices were processed with the avidin-biotin-peroxidase method (Horikawa and Armstrong 1988) to visualize biocytin-filled cells and Nissl-counterstained (Paxinos and Watson 2005). Six properly stained neurons were reconstructed using Neurolucida software (Microbrightfield, Williston, VT). The outlines of facial nucleus were identified by the presence of Nissl-stained neurons with large somata and were drawn for each section. Reconstructed neurons were analyzed for basic morphological properties, including soma location within the facial nucleus, soma diameter (i.e., the mean of the maximal and the minimal soma diameter), soma area, the number of dendrites, total dendritic length, and maximum dendritic field span (i.e., maximum distance between dendritic endings).

### *Data analysis*

During antidromic stimulation sessions we recorded electric signals in 50-ms time frames including a 10-ms prestimulus period, at a repetition rate of 0.5 Hz. Spike latencies were defined as the time between stimulus onset and the peak of the spike. For juxtacellular stimulation sessions electric signals and digital images were recorded in 500-ms time frames including a 150-ms prestimulus period, at a rate of 0.67 Hz. Movement angular trajectories were reconstructed from high-speed video records and from this we extracted the following parameters: whisker identity, peak deflection amplitude, latency of peak deflection relative to the spike time, and the maximum velocity during the rising and falling phases of the deflection. Peak deflection amplitude was also determined in the remainder of cases where movements were recorded at a low frame rate (50 Hz deinterlaced). A ratio of peak deflection amplitude was calculated for evoked movements involving several whiskers and qualitatively related to position of the whiskers within the whisker array ($n = 6$). Likewise, we also looked for a tendency toward difference in deflection amplitude depending on whisker position ($n = 8$). Movement angular trajectories that resulted from two or more successive spikes were analyzed to quantify the increase in peak whisker deflection depending on interspike interval (ISI). The increase in amplitude was expressed as a ratio of second peak(observed)/first peak(observed). The observed value was then compared with the expected value [second

peak(expected)/first peak(expected)] if one would assume linear summation of (averaged) single spike-evoked movements shifted in time based on the ISIs. This part of the analysis was restricted to high-speed video records and movements of sufficient amplitude ($n = 5$ neurons). In box plots, the box represents the 25th to 75th percentile, the top and bottom whiskers the minimum and maximum values, and the dark horizontal line the median. Means were compared with two-sample unpaired *t*-test. The significance level was set at $P < 0.05$.

## RESULTS

### *Antidromic identification of facial nucleus motor neurons*

Electrical stimulation of the buccal branch of the facial nerve results in whisker protraction exclusively at the ipsilateral side (Szwed et al. 2003). At the same time an antidromic signal is generated that can be picked up in the facial nucleus (Fig. 1, *A* and *B*, *top trace*). In 3- to 6-wk-old rats we have found this signal in >95% of all experiments. Post hoc histological analysis confirmed that an abrupt temporal change in LFP within 4 ms poststimulus signaled that the pipette tip has penetrated the facial nucleus. Accordingly we identified the dorsal border of the facial nucleus by a small "early" LFP emerging at a depth around 7.5 mm (range: 7.0–7.9 mm; at 2.4 mm lateral and 10.5 mm posterior to bregma). The maximum amplitude of the LFP was found at a depth around 7.9 mm (range: 7.3–8.3 mm; amplitude 2 mV, range: 0.1–4.6 mV). The signal disappeared at a depth around 8.2 mm (putative ventral border, range: 7.3–8.7 mm). Single motor neurons were identified by their prominent antidromic spikes superimposed on the "early" LFP (Fig. 1*B*, *middle* and *bottom traces*). Spikes that grew larger in size, i.e., >2 mV peak to peak, indicated the juxtacellular configuration was established, i.e., a direct contact between the pipette tip and the cell (Pinault 1996). Furthermore, the signal became noisier. Spike polarity was opposite to the LFP (population spike) signal. The average antidromic spike latency for all motor neurons was 2.1 ms (Fig. 1*C*; range: 1.46–3.95 ms). Once a neuron was identified by an antidromic spike we tried to evoke action potentials in response to depolarizing current pulses that were 150–200 ms in duration (Fig. 1*D*). The amount of current required to evoke an action potential was variable, ranging from <1 to >20 nA. Spike amplitude ranged from 2.2 to 51.4 mV, with an average of 13 mV. We were unable to detect secondary spikes (22 neurons, 1,025 trials with spike activity). For some neurons, noise levels were relatively high during the current pulse (Rae and Levis 2002). A typical problem was the occurrence of abrupt DC shifts during the applied current pulse that may obscure events of smaller amplitude. Thus in a fraction of our recordings we cannot exclude the possibility that secondary units <1 mV in size would have remained undetected.

### *Ongoing activity*

Most units showed no or very low spontaneous spike activity. Some units showed damage-related spike activity that resulted in whisker movements. Most spontaneous whisker movements were slow and of relatively small amplitude. In some cases we observed a high-frequency/small-amplitude whisker tremor.

### *Whisker protraction*

Figure 2 shows an example of a cell whose spikes evoked whisker protraction that was mainly but not exclusively confined to a single whisker. This was the most common evoked movement pattern observed. Figure 2*A* shows a schematic of the rat's face and the position of several whiskers whose movements were tracked with a high-speed camera (1,000 frames/s). The neuron was a large motor neuron situated in the lateral facial nucleus. The dendrites extended well beyond the facial nucleus into the reticular formation. The axon originated from a primary dendrite, no local collaterals were detected, and the axon could be traced into the fasciculated nerve bundle that continues into the facial nerve (Fig. 2*B*). Following a single current pulse evoked spike, whisker B4 began to move forward 6 ms after the spike and the whisker reached its maximum deflection of 3.0° within 21 ms (Fig. 2*C*; Supplemental Movie S1).[1] Like whisker B4, whisker B3 also moved forward virtually synchronously, but with much smaller amplitude (Fig. 2*C*, maximum deflection 0.3°). Other whiskers did not show significant movements. Also, no movements were evoked in two trials when the current pulse failed to evoke spikes (Fig. 2*D*). Movements were time-locked to the spikes, not to the onset or offset of the current pulse. In the case of multiple spikes, every spike was followed by a whisker deflection, resulting in a larger overall deflection when the ISI was relatively short (Fig. 2*E*). Given the large difference between best and second-best whisker in movement amplitude we classified this cell as a single whisker protraction cell. We classified cells as "single whisker" where the second-best whisker did not reach 20% of the best-whisker movement amplitude or where the movement of best whisker was visible and movements of other whiskers were not visually detectable. The whisker protraction movement trajectories contain several subpeaks, which are found at constant latencies. As a consequence, subpeaks are also apparent in the averaged movement trace. The average subpeak interval is 9.9 ms. The observed subpeaks may be due to mechanical resonance of the whisker as shown in Supplemental Fig. S1.

### *Whisker retraction*

Figure 3 shows an example of a whisker retraction (of the γ straddler as depicted in Fig. 3*A*) following a single evoked action potential. The whisker movement was tracked at 502 frames/s. The motor neuron was situated in the dorsocentral region of the facial nucleus (Fig. 3*B*). The whisker began to move backward 5 ms after evoking an action potential and reached its maximum deflection of 0.64° within 15 ms (Fig. 3*C*, *top traces*; Supplemental Movie S2). With respect to protraction movements, every spike was followed by a whisker deflection and whisker deflections from successive spikes merged completely when the ISI was sufficiently short (Fig. 3*E*). Moreover, no movements were evoked in any of the trials when the current pulse failed to evoke spikes (Fig. 3*D*, *bottom traces*, $n = 5$). Movements were time-locked to the spikes, not to the onset or offset of the current pulse.

### *Whisker movement classification*

The classification of movement types for all stimulated neurons is shown in Fig. 4. Of 44 stimulated neurons, 22

[1] The online version of this article contains supplemental material.

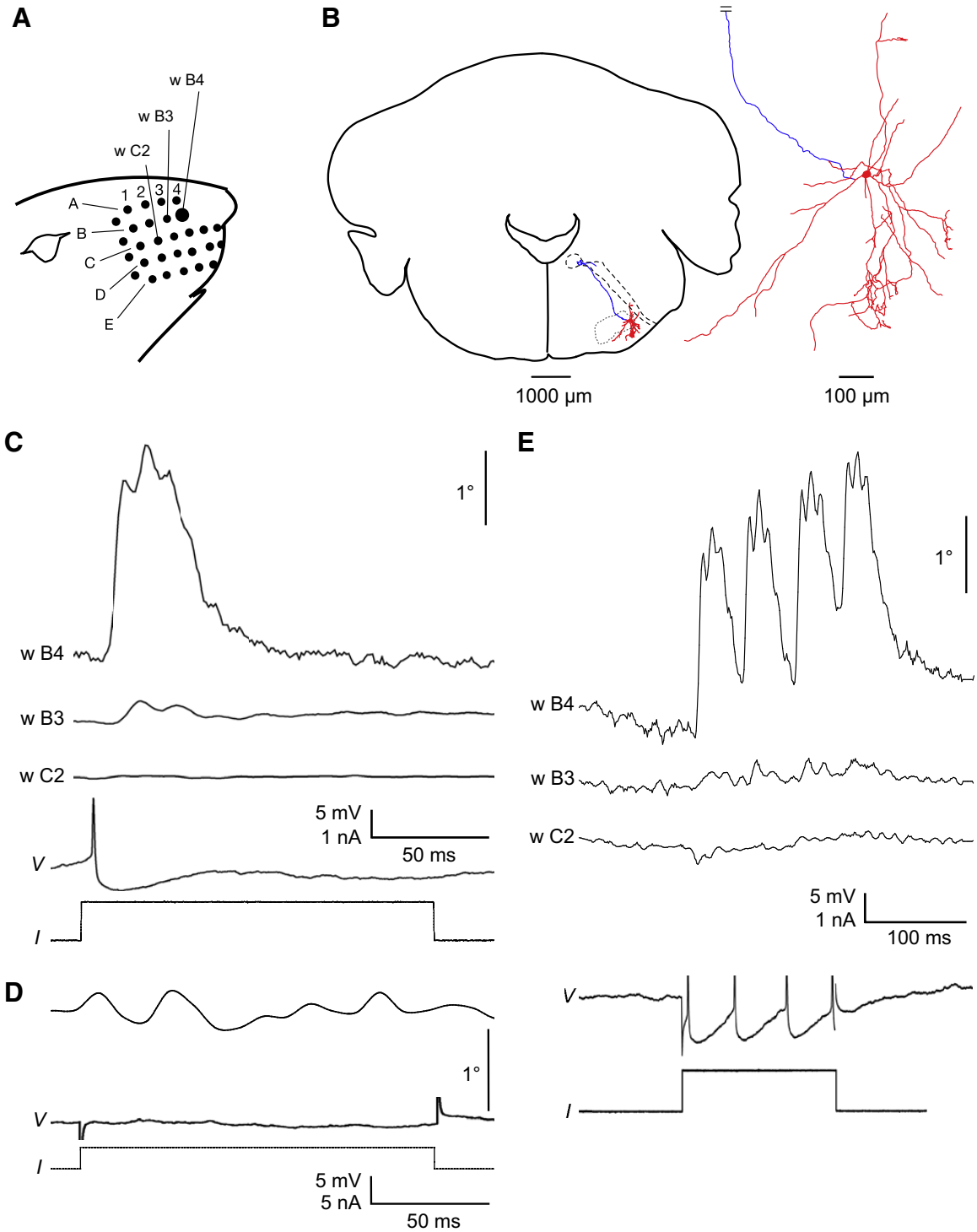


FIG. 2. Example of whisker protraction caused by single and multiple spikes. *A*: position of whisker B4 in the mystacial pad. *B*, *left*: camera lucida reconstruction of the labeled neuron with brain stem indicated. The neuron is located in the lateral part of the facial nucleus. The outline of the facial nucleus is shown as a dotted line; the efferent bundle is indicated by a dashed line. *Right*: high-magnification view of the neuron. Dendrites are shown in red; the axon is shown in blue. *C*: trajectories of whiskers B4, B3, and C2 together with the voltage (*V*) and current (*I*) signals. Following a single evoked spike, whisker B4 protracts with the highest amplitude; the movement of adjacent whisker B3 is much smaller. Whisker C2, which is in a different whisker row, does not move. *D*: no movements are seen when the current pulse fails to evoke an action potential. This movement trace was captured at a 25-Hz frame rate. *E*: movement trajectories (*top*) of whiskers B4, B3, and C2 evoked by multiple spikes (*bottom*).

neurons did not evoke any visible (whisker) movements. Stimulation of the other 22 neurons resulted in protraction of one or more whiskers, in whisker retractions, or in "combined movements." The most common movement type observed was single whisker protraction (according to the definition given earlier). Multiwhisker protractions were limited to neighboring whiskers in a single row. For the pair of whiskers with the highest amplitude we calculated a ratio

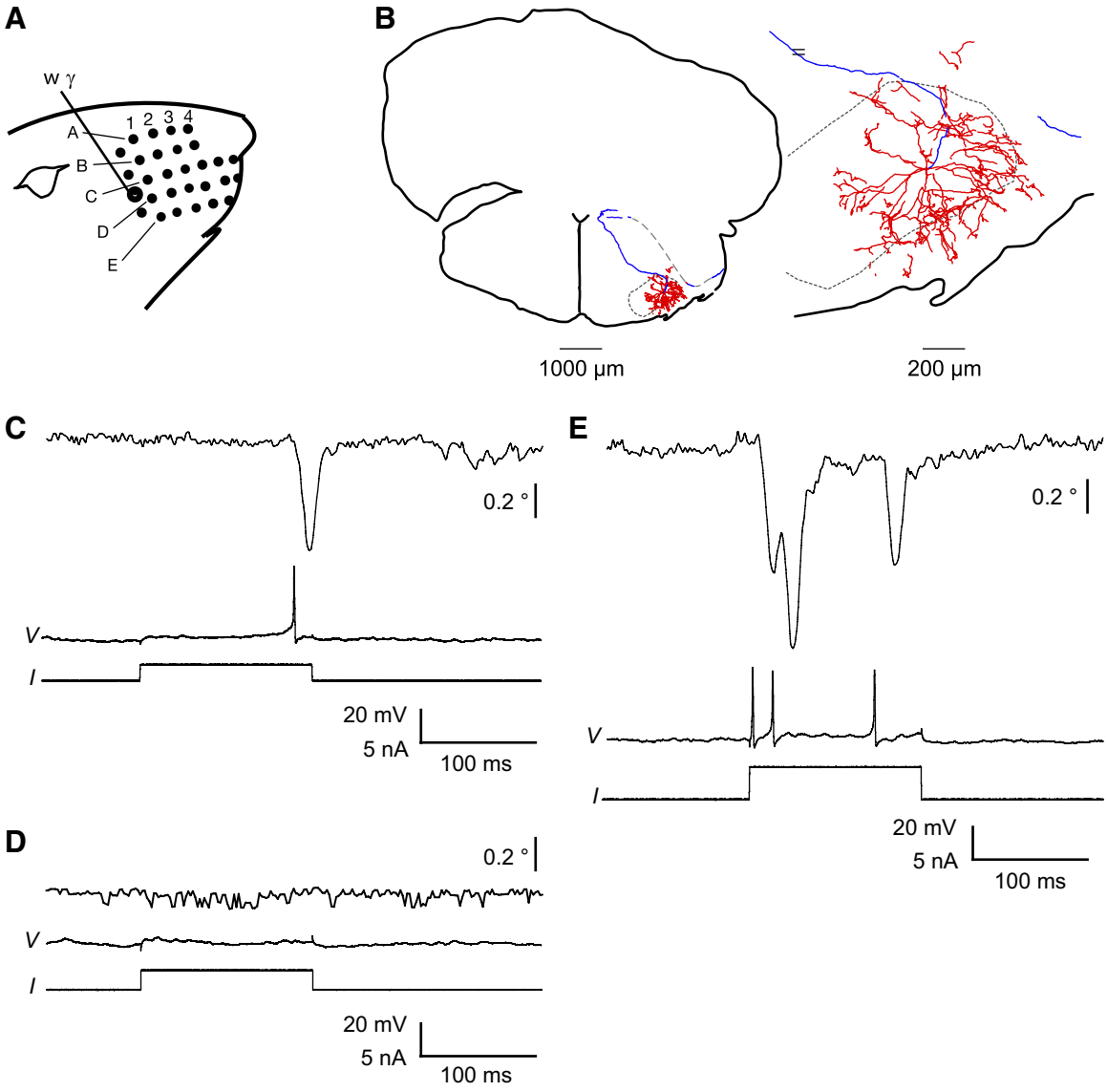


FIG. 3. Example of whisker retraction caused by single and multiple spikes. *A*: position of γ straddler in the mystacial pad. *B*: camera lucida reconstruction. The neuron is located in the intermediate subdivision of the facial nucleus. The outline of the facial nucleus is shown as a dotted line; the efferent bundle is indicated by a dashed line. *Right*: high-magnification view of the neuron. Dendrites are shown in red; the axon is shown in blue. *C*: trajectory showing retraction of γ straddler caused by a single evoked spike together with the voltage (*V*) and current (*I*) signals. *D*: no movements are seen when the current pulse fails to evoke an action potential. *E*: movement trajectory (*top*) evoked by multiple spikes (*bottom*).

of the amplitudes. The anterior/posterior whisker movement amplitude ratio varied strongly (range: 0.15–4.6; median = 1.49, $n = 6$). We did not observe a trend between amplitude ratio and whisker location in the whisker pad, i.e., neither between rows nor between different arcs. Likewise, there was no clear tendency of difference in amplitude across rows or arcs ($n = 8$). Although 80% of neurons were identified by antidromic stimulation (Fig. 1*B*), some neurons could not be activated antidromically, even when the facial nerve was stimulated with threefold the amount of current required to give a maximum response in LFP. Probably these neurons were not motor neurons. They were detected based on a change in pipette resistance and an increased noise level of the antidromic signal. They were identified as neurons by the fact that spikes were evoked by juxtacellular stimulation.

### *Movement amplitude and kinetics*

We quantified whisker movements characteristics and found that protraction amplitudes were significantly larger than retraction amplitudes (1.8 vs. 0.3°, Fig. 5*A*; Table 1). The distributions of single spike-evoked movement amplitudes were slightly skewed (Fig. 5*A*; protraction: skewness = 1.3, $P = 0.061$; retraction: skewness = 1.15, $P = 0.25$). Almost all of the evoked movements had fast kinetics. We therefore restricted our analysis of movement kinetics to those six cells, whose evoked movements were tracked with a high-speed camera. Onset of the movement occurred at 7.6 (SD 2.5) ms after the spike and the time to peak deflection was 18.2 (SD 4.3) ms (averages across all cases). Furthermore, we found a positive correlation between the maximum deflection (peak) amplitude and the maximum whisker velocity (Fig. 5*B*; Table 1). No significant correlation was found between peak ampli-

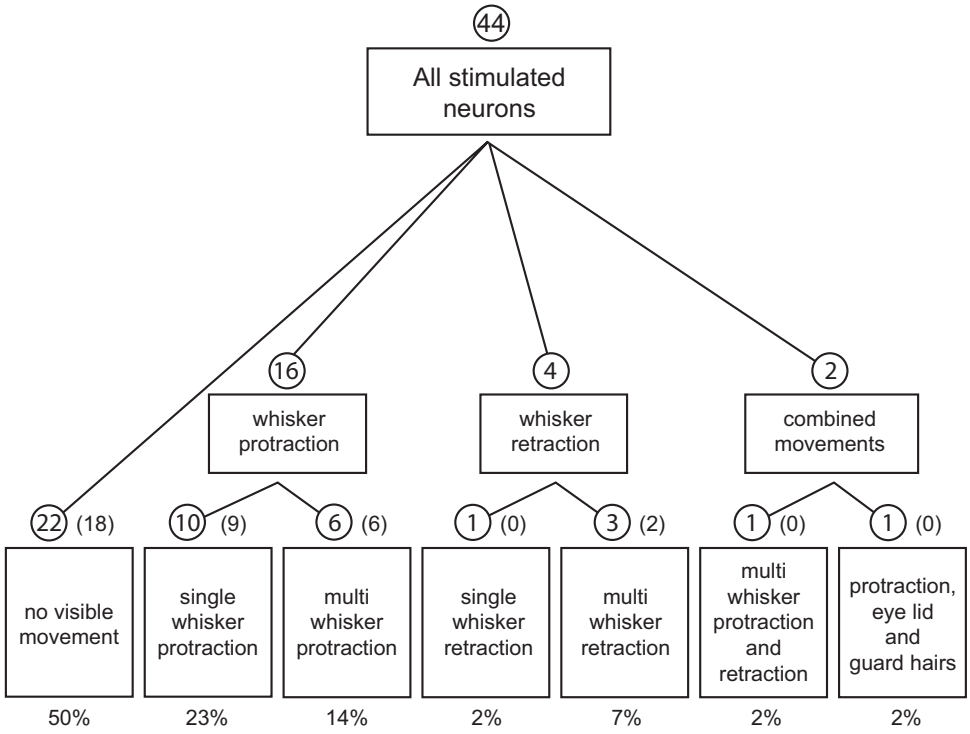


FIG. 4. Whisker movement classification scheme. The number of neurons is indicated for each class (open circles, percentage indicated below classes). The number of motor neurons within each category confirmed by antidromic activation from the facial nerve is shown in parentheses.

tude and peak latency; i.e., peak latency was relatively constant for all neurons observed, irrespective of deflection amplitude. Furthermore, average peak latency for protraction was not significantly different from that in the retraction group.

*Movements evoked by multiple successive spikes*

Next, we examined whisker movements that resulted from successive spikes and analyzed how movement amplitude was related to the ISI. Whisker deflections from successive spikes merged when ISI was relatively short, resulting in a larger overall deflection (Fig. 6, *A* and *B*). To compare whisker deflections from different experiments we normalized whisker deflection amplitude to the deflection amplitude of single spike events (ISI >1,500 ms). Maximum deflection amplitude significantly differed from unity when the ISI was <20 ms (Fig. 6*B*). Next, we investigated whether the whisker deflections could be thought of as a linear superposition of single spike-evoked movements. We found that superposition of whisker movements seems to be linear in some cases ($n = 3$; protraction movements; ISI ranges: 21.8–72.6, 17–75, 46–186) and supralinear in others ($n = 2$ neurons; one protraction and one retraction movement; ISI ranges: 11.8–70.2, 6–21.5, respectively). An example of linear summation is shown in Fig. 6, *C* and *D*. The observed peak ratio was similar to (or slightly smaller than) the peak ratio that would have been expected if linear summation is assumed ($P = 0.10$). In another case summation was significantly supralinear, i.e., peak ratio was significantly larger than expected (Fig. 6, *E* and *F*; $P = 4.7 \times 10^{-6}$; protraction movement). Supralinear summation was most pronounced at short ISI (i.e., <20 ms).

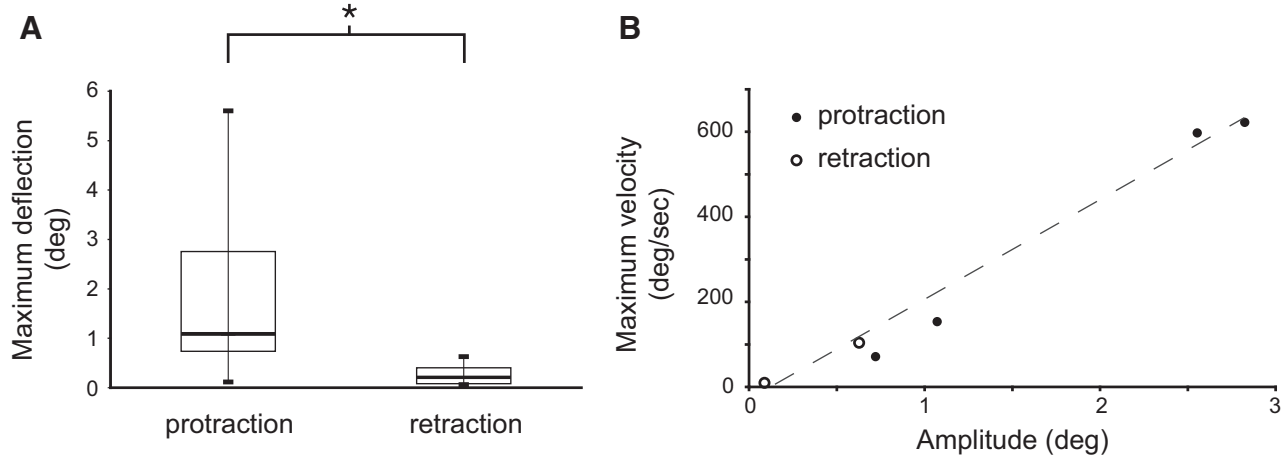


FIG. 5. Properties of single spike-evoked whisker movements. *A*: whisker protraction amplitudes are significantly larger than whisker retractions ($P < 0.05$, 2-sample unpaired *t*-test). *B*: a positive correlation is found between the maximum velocity during the rising phase (contraction phase) of the movement and the peak amplitude ($r = 0.98$, $P < 0.001$). This analysis was restricted to those neurons ($n = 6$), where movements were tracked with a high-speed camera.

TABLE 1. *Main parameters of single-spike–evoked whisker protraction and whisker retraction trajectories*

| Property | Movement Type | Neurons (*n*) | Range | Average (SD) |
|---|---|---|---|---|
| Onset latency, ms | Protraction | 4 | 4.0–9.4 | 6.7 (2.3) |
| | Retraction | 2 | 7.6, 11.1 | 9.4 |
| Peak latency, ms | Protraction | 4 | 12.3–21.1 | 17 (3.6) |
| | Retraction | 2 | 16.3, 24.7 | 20.5 |
| Max. velocity at rising phase, °/s | Protraction | 4 | 71–618 | 360 (288) |
| | Retraction | 2 | 9, 104 | 57 |
| Max. velocity at falling phase, °/s | Protraction | 4 | 60–391 | 187 (149) |
| | Retraction | 2 | 9, 83 | 46 |
| Amplitude | Protraction | 10 | 0.12–5.6 | 1.8 (1.7) * |
| | Retraction | 4 | 0.06–0.63 | 0.28 (0.26) * |

SDs are shown in parentheses. *$P < 0.05$, two-sample *t*-test, assuming unequal variances.

*Movement reliability and variability*

All facial motor neurons in our data set that gave rise to spike-evoked whisker movements did so faithfully. We did not observe any instances of movement failures (22 neurons, 1,025 trials with spike activity, $P < 0.001$). Conversely, no movements were observed that were time-locked to the current pulse in any of the trials where the motor neuron did not reach its spiking threshold. Figure 7 illustrates such reliability for single spike-evoked whisker protractions. In 472 of 815 trials no spike was evoked; no movements were observed in these cases. In the remainder of trials, we observed 61 single spike and 282 multispike evoked whisker movements. Variability of single spike-evoked movements was low and could be attributed largely to spontaneous background movements with a

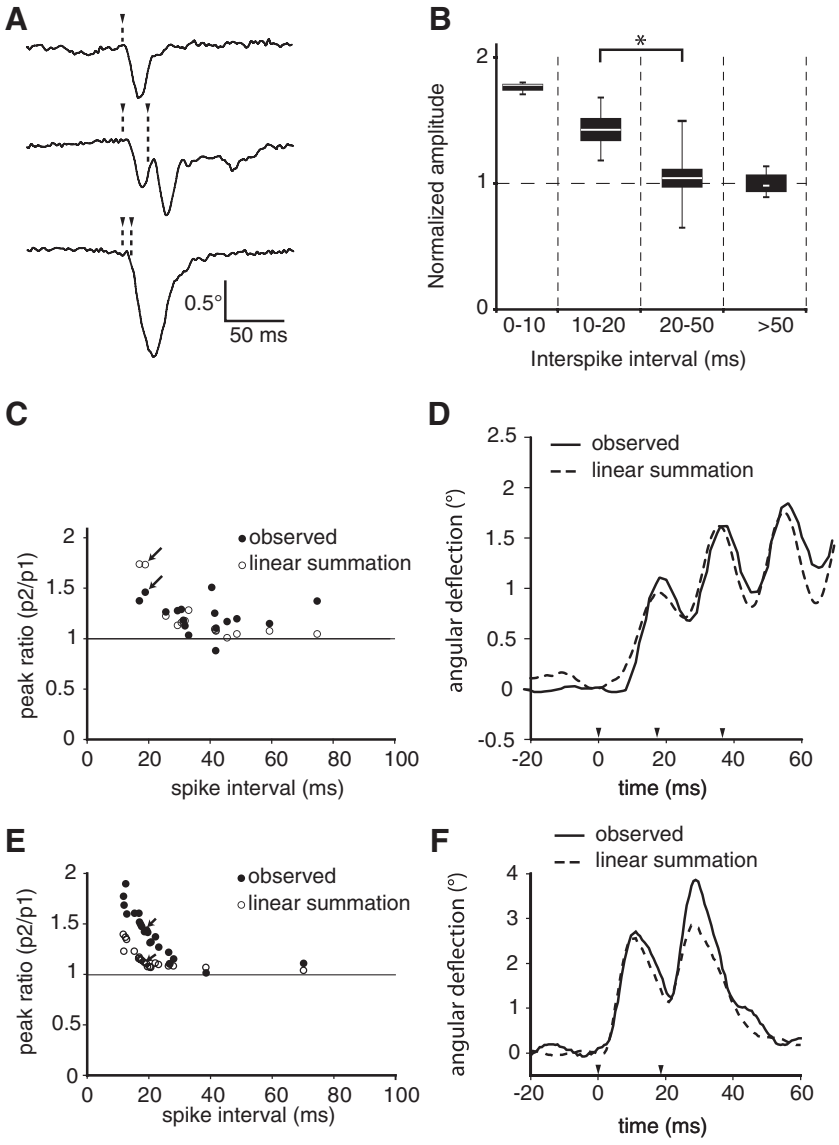


FIG. 6. Movement effects of successive spikes. *A*: whisker position traces and spike times (dashed lines with triangles). *Top trace*: single spike-evoked movement. *Middle trace*: 2 spikes with intermediate interspike interval (ISI = 21.4 ms) give rise to a deflection pattern with 2 distinguishable subpeaks. *Bottom trace*: with shorter ISI (7.4 ms) the subpeaks completely merge into one larger peak. *B*: population statistics for dependence of maximum deflection on ISI (5 neurons). *C*: example of linear movement summation. The observed peak ratios are similar to the expected peak ratio indicating linear summation. *D*: whisker position trace corresponding to the datapoints indicated by arrows (*C*; ISI = 18.9 ms). Summation seems to be linear also at relatively short ISI. *E*: example of supralinear summation. The observed peak ratios are significantly larger than expected, especially at short ISI. *F*: whisker position trace corresponding to the datapoints indicated by arrows (*E*; ISI = 18.5 ms). Spike times are indicated by triangles.

frequency centered around 70 Hz. The origin of this movement is unclear at this point. The movement might spontaneously occur in natural conditions at low amplitude. Alternatively, it may be due to neuronal damage resulting in fast spiking patterns or it may be due to side effects of anesthesia. Evoked whisker movements were not phase-locked to the spontaneous background movements. The SDs of peak latency and peak amplitude were 0.7 ms and 0.23°, respectively (Fig. 7).

### *Complex movements*

In two neurons spikes evoked combined movements. These cells could not be antidromically activated and thus were probably not motor neurons. Action potentials in one of them resulted in simultaneous whisker protractions in whisker D-row and whisker retractions in whisker E-row. Whisker movements were tightly coupled to the evoked spikes (Supplemental Movie S3). Evoked action potentials in the other neuron gave rise to combined whisker protractions, eye lid twitch, and guard hair movements. Possibly, part of the innervation is not restricted to one particular muscle group, but involves separate muscle groups (Supplemental Movie S4).

### *Motor neuron morphology and localization*

Six neurons were recovered and reconstructed; one was related to whisker protraction, two were related to whisker retraction, and the remaining three were from the nonmovement class. Soma diameter averaged 30 $\mu$m and neurons had 6–14 primary dendrites running in all directions, some of them extending outside the nuclear boundary (Table 2). Dendrites extended beyond the boundaries of the facial nucleus in dorsal and ventral direction and to a lesser extent in the lateral direction; no dendritic arbors were found medial of the facial nucleus. Average total dendritic length was 25.8 mm and the maximum dendritic field span was 1.2 mm (Table 2). Three somata were located in the middle third part of the facial nucleus [related to whisker retraction ($n = 2$) and no movement ($n = 1$)] and three somata in the lateral third part [whisker protraction ($n = 1$) and no movement ($n = 2$)]. Somata from neurons that gave rise to whisker retractions were located relatively close to the dorsal boundary of the facial nucleus. No local axon collaterals were seen as far as the axons could be traced.

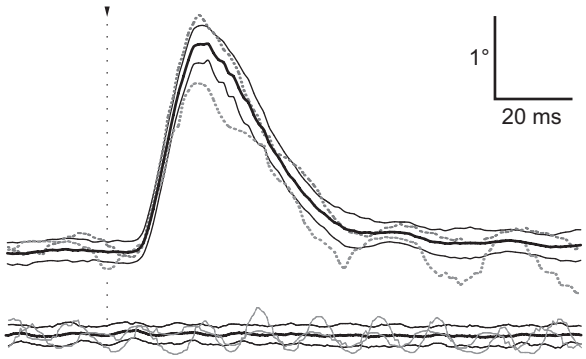


FIG. 7. Reliability and movement variability. Average movement profile (thick line) with ±1SD boundaries (thin lines). Movements are aligned relative to the spike time (triangle). The minimum and maximum amplitude movement profiles (dashed lines) are within normal range, considering the pronounced ongoing high-frequency whisker tremor, i.e., these cases are not identified as outliers (Moore and McCabe 1999). Whisker movements are absent when spikes are absent (*bottom*).

## DISCUSSION

### *Juxtacellular stimulation activates single facial nucleus neurons*

Our conclusions rest on the assumption that our juxtacellular stimulation technique consistently activated single facial nucleus neurons. A number of observations support this idea. *1*) Juxtacellular stimulation did evoke movements when spikes were fired. *2*) In cells, where spike-evoked movements were observed, every spike evoked a movement. *3*) Juxtacellular stimulation did not evoke movements when no spikes were fired. *4*) Evoked movements were tightly time-locked to evoked spikes but were not tightly time-locked to the onset of current injections. *5*) Stimulation currents were very small (in the nanoampere range), far smaller than the microstimulation currents (in the microampere range) that were required to activate neurons and whisker movements by conventional extracellular stimulation. *6*) Consistent with previous work (Pinault 1996) our staining attempts resulted in the staining of single neurons. *7*) Spikes of the stimulated neuron had large amplitude (13 mV on average) and had a unimodal amplitude distribution, whereas no secondary spikes were detected. *8*) A recent study in barrel cortex reached a similar conclusion (Houweling and Brecht 2008).

### *General movement characteristics*

We observed that each spike of facial nucleus neurons evoked a stereotyped movement most often of a single whisker. The vast majority of cells caused either protraction or retraction movements; i.e., the movement direction depended on the identity of the stimulated neuron. The characteristics of movements evoked by the facial nucleus neuron stimulation are thus very different from the characteristics of movement evoked by vibrissa motor cortex neuron stimulation, where complex, several-seconds-long multiwhisker movement sequences are evoked (Brecht et al. 2004).

### *Variety of movement types*

In the movements evoked by facial nucleus neuron stimulation, protraction dominated over retraction. This may reflect the fact that a significant percentage of the motoneurons in the lateral facial subnucleus innervate only intrinsic follicle muscles (Klein and Rhoades 1985). Active whisker protraction might be biologically more important than active whisker retraction. *1*) The intrinsic whisker muscles, which subserve protraction, form the lion's share of the whisker musculature. *2*) Protraction is the part of the whisking cycle that leads to whisker contacts with objects in front of the animal. *3*) "Passive processes" (i.e., elasticity and muscular relaxation) might critically contribute to whisker retraction (Dörfl 1982). Studies in rats (Berg and Kleinfeld 2003a) and hamsters (Wineski 1985) have shown that extrinsic muscle groups are involved in active retraction. In protraction movements single-whisker movements dominated (10 of 16), whereas a majority of spike-evoked whisker retractions (3 of 4) involved more than one whisker. These movement characteristics match well with

TABLE 2. *Morphological characteristics of motor neurons in the rat facial nucleus*

| Property | All Motor Neurons ($n$ = 6) | Protraction ($n$ = 1) | Retraction ($n$ = 2) | No Movement ($n$ = 3) |
|---|---|---|---|---|
| Soma diameter, $\mu$m | 30 (8.9) | 21.6 | 31.6 (40, 23) | 29.4 (12.7) |
| Soma area, $\mu m^2$ | 562 (302) | 344 | 590 (871, 308) | 593 (447) |
| Number of dendrites | 8.3 (2.9) | 7 | 10.5 (14, 7) | 7.3 (1.2) |
| Total dendritic length, $\mu$m | 25,753 (19,765) | 9,169 | 48,325 (38,202, 58,448) | 16,234 (9,550) |
| Maximum dendritic field span, $\mu$m | 1,193 (328) | 1,102 | 1,435 (1,674, 1,196) | 1,061 (350) |

Values are means (SD) or individual values.

the anatomy of the whisker musculature. Intrinsic whisker muscles are arranged as slings around individual whisker follicles and thus enable the protraction of single whiskers (Dörfl 1982). The origin of multiwhisker protraction is unclear at this point. The intrinsic whisker muscles are spatially well isolated from one another. The anchoring or contacting of the intrinsic muscle sling on the neighboring same row, more posterior whisker may impose some torque on that whisker, resulting in synchronized protraction of a pair of whiskers located in the same row. Depending on the distance between the whiskers pivot point and intrinsic muscle anchoring point (Berg and Kleinfeld 2003a), movement amplitude may be negligible or reasonably large compared with the anterior whisker's amplitude. We think it is unlikely that events of two or even more whiskers moving in synchrony can be explained by passive movement transfer via connective tissue in between whisker follicles since both anterior and posterior whiskers within a single row have been found to move with the largest amplitude. Moreover, the range of deflection amplitude ratio encountered was large (0.15–4.6) and did not seem to be correlated with position in the whisker pad. Another explanation would be that multiwhisker movements are due to additional stimulation of adjacent neurons (Pinault 1996), but as discussed earlier our data are inconsistent with such a scenario. Other possible explanations are electrical coupling between motor neurons that would allow for synchronized activity of adjacent motor neurons (Rekling and Feldman 1997) or, alternatively, the presence of axon-collaterals branching to intrinsic muscles of different whiskers (Streppel et al. 2002). The extrinsic muscles anchor to the skin external to the whisker pad and run below the skin in thin bundles (Dörfl 1982; Jin et al. 2004). As a consequence, extrinsic muscle contractions and the resulting whisker retractions usually involve multiple whiskers. It is not entirely obvious how retraction of a single whisker occurs. Two possibilities are *1*) single whisker retraction occurs via the activation of a single-whisker retraction motor neuron, even though such cells seem to be rare according to our data; and *2*) single-whisker retraction could perhaps also be mediated through the inhibition of a tonically active protraction neuron.

### *Absence of evoked movements in a large fraction of facial nucleus neurons*

A surprising finding was that about 50% of all neurons that were identified by an antidromic spike did not give rise to detectable whisker movements. It is possible that neurons generated isometric muscle contractions without overt movement.

### *Movement amplitude*

One finding of particular interest is that we found a large range in movement amplitude, for both the protraction and the retraction movement classes (Fig. 5). A large range in movement amplitude might be ascribed to differences in motor unit size (Enoka and Fuglevand 2001), differences in electrical coupling (Rekling and Feldman 1997), or the presence of axon-collaterals (Angelov et al. 2005). The location of the motor unit may also affect whisker movement amplitude. Movement direction depended on the identity of the stimulated neuron. This is very different from movements evoked by single-neuron stimulation in vibrissa motor cortex, where movement direction (and amplitude) depended on spike frequency and depth of anesthesia (Brecht et al. 2004). The movement amplitudes we observed were on average 1.8° for protraction (cells for which no movement could be evoked excluded). On average, episodes of natural whisking protraction movements have amplitudes of about 60° and a protraction continues for about 60 ms (Kleinfeld et al. 1999). In our present study it proved to be difficult to fire facial nucleus neurons at rates $\gg$100 Hz. Thus a single facial nucleus neuron is unlikely to contribute more than about five spikes, which would result in a 9° protraction (assuming average movement amplitudes) to such a movement. From this one can estimate a lower limit of 7 neurons to be active at a single whisker protraction (i.e., 60°/9°), when assuming linear movement summation. A higher limit of neurons active per single whisker protraction would then be 60°/1.5° = 40 neurons, when each neuron generates a single action potential. These considerations make it likely that many facial nucleus neurons contribute to a simple whisker movement and—since there are only 50–100 neurons per whisker—we guess that several tens of percent of facial nucleus cells contribute to large movements. The situation in the facial nucleus is very different from that in vibrissa motor cortex, where single-cell–evoked movement amplitudes were also about 1°, but which contains nearly 30,000 neurons per whisker and where one would therefore think that only a very small fraction of cells can generate large movements (Brecht et al. 2004). Single-cell–evoked movement effects from motor cortex may last for several seconds after the stimulus and movements are slow. It appears that single cortical neurons activate a few motor neurons repetitively over several seconds. This divergence of the cortical motor command could occur via a brain stem pattern generator.

### *Movement kinetics*

We observed that stimulation leads to prompt whisker movements, whereby the kinetics of each particular movement

depended on the identity of the stimulated neuron. The speed of the large-amplitude whisker movements evoked by facial nucleus stimulation exceeds by far the speed of movements observed after single-neuron stimulation in vibrissa motor cortex (Brecht et al. 2004). The protraction and retraction movements share several characteristics: both are fast movements that have comparable movement onset latency and peak latency relative to the spike time. Movement parameters have a low variability from cell to cell and from trial to trial. The relaxation phase of the movement also seems similar. As a result, the protraction and retraction movements seem to be well matched in their kinetic properties, despite the fact that different muscle classes are involved that act in a different way on the angular position of the whisker (Dörfl 1982; Wineski 1985). The peak latency is relatively constant for all neurons observed, irrespective of deflection direction and amplitude. Consequently, movement amplitude was positively correlated with maximum angular velocity.

### *Movements evoked by multiple successive spikes*

Based on an anatomical study by Dörfl et al., Berg and Kleinfeld (2003b) constructed a mechanical model that relates vibrissa movements to the underlying alternating muscle contractions of the intrinsic and extrinsic muscle groups. From the analysis of movements evoked by multiple successive spikes we conclude that motor units are heterogeneous with respect to the degree of nonlinearity of muscle twitch summation. We observed nonlinear summation for both whisker protractions and whisker retractions.

### *Complex movements*

We classified two observations as "combined movements." In both cases cells were not antidromically activated, but the neurons were most probably localized close to or within boundaries of the facial nucleus as inferred from the antidromic local field response. It is unclear how these complex movements are generated.

### *Cell morphology*

The somadendritic morphology of facial motor neurons has been extensively described, using horseradish peroxidase in intracellular recordings (Friauf 1986), and our findings agree with these data.

### *A labeled line/spike-by-spike code for whisker movements in the facial nucleus*

A synopsis of our findings suggests the following coding scheme for whisker movements in the facial nucleus. *1*) Evoked movement characteristics depend on the identity of the stimulated neuron (a labeled line code). *2*) The facial nucleus neurons are heterogeneous with respect to the movement properties they encode. *3*) Facial nucleus spikes are translated in a one-to-one manner into whisker movements. Movements were reliably evoked and stereotyped and movement summation may be either linear or supralinear. This spike-by-spike coding of movements by the facial nucleus is very different from the vibrissa motor cortex, where movements are encoded by spike sequences. Specifically, in cortex movement latency depends on spike number, whereas movement amplitude and direction depend on spike frequency (Brecht et al. 2004). All neural processing in the context of vibrissal motor control therefore converges in the facial nucleus to a very simple spike-by-spike code. In turn, the well-established characteristics of neuromuscular transmission (Katz 1966)—reliability, speed, stereotypy—are perfectly suited to account for the movement characteristics observed here. Single-neuron stimulation is a powerful approach for understanding neural movement control because it explicitly allows determination of how individual neurons represent movements. We reason that the single motor-neuron–evoked movements described here form an elementary "motor alphabet" for whisker movements, from which upstream motor centers synthesize the animal's whisker movement repertoire.

## ACKNOWLEDGMENTS

We thank K. Donkersloot and R. Herfst for developing the whisker tracking software and H. van der Burg and E. Haasdijk for technical assistance; J. Epszstein, A. Houweling, A. Lee, B. Voigt, and C. Roth-Alpermann for reading the manuscript; and J. Wolfe for clarifying the role of whisker resonance in evoked movements.

## GRANTS

This work was supported by a European Union (EU) Sensopac grant, an EU Biotact grant, the Bernstein Center for Computational Neuroscience at Humboldt-University Berlin, and a Netherlands Organisation for Scientific Research VIDI grant and a Human Frontier Science Program grant to M. Brecht.

## REFERENCES

**Ahrens KF, Kleinfeld D.** Current flow in vibrissa motor cortex can phase-lock with exploratory rhythmic whisking in rat. *J Neurophysiol* 92: 1700–1707, 2004.

**Angelov DN, Guntinas-Lichius O, Wewetzer K, Neiss WF, Streppel M.** Axonal branching and recovery of coordinated muscle activity after transection of the facial nerve in adult rats. *Adv Anat Embryol Cell Biol* 180: 1–130, 2005.

**Berg RW, Kleinfeld D.** Rhythmic whisking by rat: retraction as well as protraction of the vibrissae is under active muscular control. *J Neurophysiol* 89: 104–117, 2003a.

**Berg RW, Kleinfeld D.** Vibrissa movement elicited by rhythmic electrical microstimulation to motor cortex in the aroused rat mimics exploratory whisking. *J Neurophysiol* 90: 2950–2963, 2003b.

**Brecht M, Grinevich V, Jin TE, Margrie T, Osten P.** Cellular mechanisms of motor control in the vibrissal system. *Pfluegers Arch* 453: 269–281, 2006.

**Brecht M, Preilowski B, Merzenich MM.** Functional architecture of the mystacial vibrissae. *Behav Brain Res* 84: 81–97, 1997.

**Brecht M, Schneider M, Sakmann B, Margrie TW.** Whisker movements evoked by stimulation of single pyramidal cells in rat motor cortex. *Nature* 427: 704–710, 2004.

**Carvell GE, Simons DJ.** Biometric analyses of vibrissal tactile discrimination in the rat. *J Neurosci* 10: 2638–2648, 1990.

**Carvell GE, Simons DJ.** Task- and subject-related differences in sensorimotor behavior during active touch. *Somatosens Mot Res* 12: 1–9, 1995.

**Cramer NP, Li Y, Keller A.** The whisking rhythm generator: a novel mammalian network for the generation of movement. *J Neurophysiol* 97: 2148–2158, 2007.

**Dörfl J.** The musculature of the mystacial vibrissae of the white mouse. *J Anat* 135: 147–154, 1982.

**Enoka RM, Fuglevand AJ.** Motor unit physiology: some unresolved issues. *Muscle Nerve* 24: 4–17, 2001.

**Friauf E.** Morphology of motoneurons in different subdivisions of the rat facial nucleus stained intracellularly with horseradish peroxidase. *J Comp Neurol* 253: 231–241, 1986.

**Haiss F, Schwarz C.** Spatial segregation of different modes of movement control in the whisker representation of rat primary motor cortex. *J Neurosci* 25: 1579–1587, 2005.

**Hall RD, Lindholm EP.** Organization of motor and somatosensory neocortex in the albino rat. *Brain Res* 66: 23–38, 1974.

**Hattox A, Li Y, Keller A.** Serotonin regulates rhythmic whisking. *Neuron* 39: 343–352, 2003.

**Hattox AM, Priest CA, Keller A.** Functional circuitry involved in the regulation of whisker movements. *J Comp Neurol* 442: 266–276, 2002.

**Horikawa K, Armstrong WE.** A versatile means of intracellular labeling: injection of biocytin and its detection with avidin conjugates. *J Neurosci Methods* 25: 1–11, 1988.

**Houweling AR, Brecht M.** Behavioural report of single neuron stimulation in somatosensory cortex. *Nature* 451: 65–68, 2008.

**Jin TE, Witzemann V, Brecht M.** Fiber types of the intrinsic whisker muscle and whisking behavior. *J Neurosci* 24: 3386–3393, 2004.

**Katz B.** *Nerve, Muscle, and Synapse.* New York: McGraw-Hill, 1966, p. ix.

**Klein BG, Rhoades RW.** Representation of whisker follicle intrinsic musculature in the facial motor nucleus of the rat. *J Comp Neurol* 232: 55–69, 1985.

**Kleinfeld D, Ahissar E, Diamond ME.** Active sensation: insights from the rodent vibrissa sensorimotor system. *Curr Opin Neurobiol* 16: 435–444, 2006.

**Kleinfeld D, Berg RW, O'Connor SM.** Anatomical loops and their electrical dynamics in relation to whisking by rat. *Somatosens Mot Res* 16: 69–88, 1999.

**Knutsen PM, Pietr M, Ahissar E.** Haptic object localization in the vibrissal system: behavior and performance. *J Neurosci* 26: 8451–8464, 2006.

**Krupa DJ, Matell MS, Brisben AJ, Oliveira LM, Nicolelis MA.** Behavioral properties of the trigeminal somatosensory system in rats performing whisker-dependent tactile discriminations. *J Neurosci* 21: 5752–5763, 2001.

**Lang EJ, Sugihara I, Llinás R.** Olivocerebellar modulation of motor cortex ability to generate vibrissal movements in rat. *J Physiol* 571: 101–120, 2006.

**Moore DS, McCabe GP.** *Introduction to the Practice of Statistics.* New York: Freeman, 1999, p. xxviii.

**Paxinos G, Watson C.** *The Rat Brain in Stereotaxic Coordinates.* Amsterdam: Elsevier Academic Press, 2005, p. xliii, 166.

**Pinault D.** A novel single-cell staining procedure performed in vivo under electrophysiological control: morpho-functional features of juxtacellularly labeled thalamic cells and other central neurons with biocytin or neurobiotin. *J Neurosci Methods* 65: 113–136, 1996.

**Porter R, Lemon R.** *Corticospinal Function and Voluntary Movement.* New York: Clarendon Press, 1993, p. xviii.

**Rae JL, Levis RA.** Single-cell electroporation. *Pfluegers Arch* 443: 664–670, 2002.

**Rekling JC, Feldman JL.** Bidirectional electrical coupling between inspiratory motoneurons in the newborn mouse nucleus ambiguus. *J Neurophysiol* 78: 3508–3510, 1997.

**Streppel M, Azzolin N, Dohm S, Guntinas-Lichius O, Haas C, Grothe C, Wevers A, Neiss WF, Angelov DN.** Focal application of neutralizing antibodies to soluble neurotrophic factors reduces collateral axonal branching after peripheral nerve lesion. *Eur J Neurosci* 15: 1327–1342, 2002.

**Szwed M, Bagdasarian K, Ahissar E.** Encoding of vibrissal active touch. *Neuron* 40: 621–630, 2003.

**Vincent SB.** The function of vibrissae in the behavior of the white rat. *Behav Monogr* 1: 7–81, 1912.

**von Heimendahl M, Itskov PM, Arabzadeh E, Diamond ME.** Neuronal activity in rat barrel cortex underlying texture discrimination. *PLoS Biol* 5: e305, 2007.

**Welker WI.** Analysis of sniffing of the albino rat. *Behavior* 22: 223–244, 1964.

**Wineski LE.** Facial morphology and vibrissal movement in the golden hamster. *J Morphol* 183: 199–217, 1985.